Environ. Sci. Technol. **2002**, *36,* 4352−4357

X-ray Absorption Spectroscopy Study of the Effects of pH and Ionic Strength on Pb(II) Sorption to Amorphous Silica

EVERT J. ELZINGA* AND DONALD L. SPARKS
Department of Plant and Soil Sciences, University of Delaware, Newark, Delaware 19717-1303

Pb(II) sorption to hydrous amorphous SiO_2 was studied as a function of pH and ionic strength using XAS to characterize the sorption products formed. Pb sorption increased with increasing pH and decreasing ionic strength. The XAS data indicated that the mechanism of Pb(II) sorption to the SiO_2 surface was pH-dependent. At pH < 4.5, a mononuclear inner-sphere Pb sorption complex with ionic character dominated the Pb surface speciation. Between pH 4.5 and pH 5.6, sorption increasingly occurred via the formation of surface-attached covalent polynuclear Pb species, possibly Pb−Pb dimers, and these were the dominant Pb complexes at pH ≥ 6.3. Decreasing ionic strength from $I = 0.1$ to $I = 0.005$ M $NaClO_4$ significantly increased Pb sorption but did not strongly influence the average local coordination environment of sorbed Pb at given pH, suggesting that the formation of mononuclear and polynuclear Pb complexes at the surface were coupled; possibly, Pb monomers control the formation of Pb polynuclear species by diffusion along the surface, or they act as nucleation centers for additional Pb uptake from solution. This study shows that the effectiveness of SiO_2 in retaining Pb(II) is strongly dependent on solution conditions. At low pH, Pb(II) may be effectively remobilized by competition with other cations, whereas sorbed Pb is expected to become less susceptible to desorption with increasing pH. However, unlike for Ni(II) and Co(II), no lead phyllosilicates are formed at these higher pH values; therefore, SiO_2 is expected to be a less effective sink for Pb immobilization than for these other metals.

Introduction

Determining the mechanisms of heavy metal retention on mineral surfaces is important in understanding and predicting the speciation, mobility and bioavailablity of these contaminants in natural environments since dissolved metal concentrations are largely controlled by solute partitioning to solid phases. Recent spectroscopic studies have shown that metal sorption to mineral phases may occur via a number of mechanisms. These include electrostatic interactions, leading to the formation of outer-sphere metal sorption complexes; chemical bonding between the metal ions and surface functional groups, leading to inner-sphere metal sorption complexes; and formation of multinuclear metal precipitate phases (*1*−*12*). Distinguishing between these mechanisms is important because they determine the stability of the partitioned metal ions. Outer-sphere complexes are relatively weakly held, and as a result, they are more susceptible to desorption than more strongly bound inner-sphere complexes. Metal precipitate phases tend to be more resistant to metal remobilization than mononuclear surface adsorption complexes and may gain additional stability over time (*13*, *14*). Moreover, since the capacity for metal retention through three-dimensional precipitation is not restricted by the number of available surface sites (which is the case for mononuclear inner- and outer-sphere surface complexation), precipitation reactions may be highly effective in retaining trace metals in aqueous systems.

In this study, we investigated Pb sorption to hydrous amorphous SiO_2. Amorphous silica is abundant in marine environments, originating mostly from skeletal remains of planktonic organisms and sponges, although it can also form as an inorganic precipitate (*15*). In the vadozone, SiO_2 is mostly present as quartz, a mineral found in essentially all soils, sediments, and parent materials. Quartz grains in soils and sediments often have clay mineral coatings, and it has been suggested that these coatings may form upon the sorption of hydrolyzable metal cations such as Mg(II), Ni(II), and Co(II) to the quartz surface (*16*). Given the abundance of quartz in soils and sediments, this (three-dimensional) precipitation mechanism may be an important mechanism of heavy metal retention in these systems, despite the relatively low surface area of quartz. Manceau et al. (*16*) indicated that interactions between metals and surfaces of quartz and amorphous silica are likely to be similar since these sorbents have a similar short-range order, with the main difference being the range of Si−O−Si bond angles present. As such, amorphous silica can be regarded as a high surface area analogue for quartz. Studying the interactions of heavy metals with the amorphous silica surface is therefore relevant to understanding the behavior of heavy metals contaminants in both marine and vadozone environments, with the high surface area of amorphous silica facilitating the use of spectroscopic techniques to study metal sorption reactions at the SiO_2 surface on a molecular level. No spectroscopic studies of Pb(II) sorption to amorphous SiO_2 have been reported in the literature, but studies of Cr(III), Co(II), Cu(II), Mg(II), and Ni(II) sorption to amorphous silica and quartz have shown the formation of multinuclear metal sorption products upon contact with these SiO_2 phases, including the formation of magnesium(II) and cobalt(II) phyllosilicates (*10*, *16*−*23*). X-ray absorption spectroscopy (XAS) investigations of Pb(II) sorption to iron(III), manganese(III, IV), and aluminum(III) oxides have shown the formation of predominantly mononuclear inner-sphere Pb complexes on these mineral surfaces (*2*−*6*). Recent spectroscopic studies have shown that system parameters such as pH and ionic strength may affect not only the extent of trace metal uptake by mineral surfaces but also the mechanism by which the metals cations are retained (*7*, *11*, *24*, *25*). The aim of this study was to investigate the mechanism of Pb sorption to amorphous silica as a function of pH and ionic strength, using XAS spectroscopy to characterize the Pb sorption products formed at the SiO_2 surface.

Materials and Methods

The hydrous amorphous SiO_2 used was Zeo49, obtained from the J. M. Huber Corporation. This silica has been used as a sorbent in previous metal sorption studies (*26*, *27*) and has a reported BET surface area of 280 $m^2\ g^{-1}$, and an average particle diameter of 9 μm (*26*). The material contains a slight Al contamination with a molar Si/Al ratio of 400 (*26*).

* Corresponding author present address: Department of Geosciences, State University of New York, Stony Brook, NY 11794-2100; phone: (631)632-9643; e-mail: eelzinga@notes.cc.sunysb.edu.

10.1021/es0158509 CCC: $22.00
Published on Web 09/14/2002

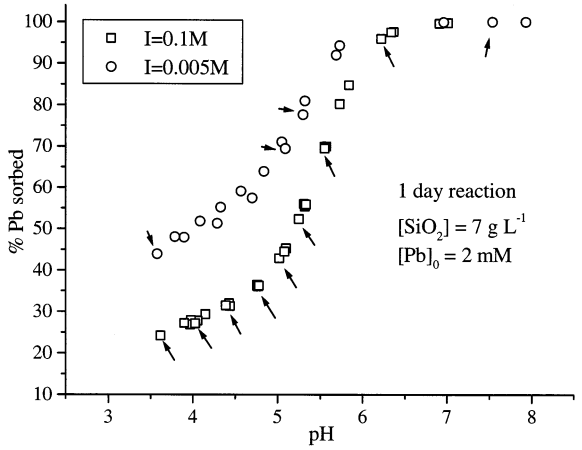

FIGURE 1. Comparison of the pH edges of Pb sorption at $I = 0.1$ and 0.005 M. The arrows denote the samples analyzed by XAS.

Batch sorption studies were performed in a N_2-purged glovebox, using boiled DDI water for sample and reagent preparation. The SiO_2 concentration was 7.0 g L^{-1}, and the initial Pb solution concentration was 2.0 mM. The experimental parameters that were varied were pH (3.6−7.5) and ionic strength ($I = 0.1$ and 0.005 M $NaClO_4$). Prior to reaction with Pb, the amorphous SiO_2 material was hydrated in the background electrolyte for 24 h at pH 4.0. Next, an appropriate amount of a 0.1 M $Pb(ClO_4)_2$ stock solution was added to achieve a Pb solution concentration of 2.0 mM. The suspension was then titrated to higher pH by stepwise addition of 0.1 M NaOH. After each pH increment, 10-mL aliquots were transferred from the main reaction vessel to 30-mL centrifuge tubes. The centrifuge tubes were placed on an end-over-end rotator operating at 25 rpm, for a reaction time of 24 h. After equilibration, the final suspension pH was measured, and the samples were centrifuged at 18000 rpm for 10 min. The supernatants were filtered through 0.22-μm filters, acidified, and analyzed for Pb using atom absorption spectrometry. The amount of Pb sorbed was calculated as the difference between the initial and the final Pb solution concentrations. Speciation calculations with MINEQL (*28*) indicated that all final solutions were undersaturated with respect to Pb precipitate phases.

Preparation of the XAS samples was done using the same procedure as described above, except that total volumes of 60 mL were used for these samples. To avoid Pb desorption, the wet pastes remaining after centrifugation were not washed to remove nonsorbed Pb in the entrained electrolyte. In the sample with the lowest Pb loading, the amount of Pb in the entrained electrolyte represented ≈3% of total Pb present in the sample, with the percentage going down to essentially 0% for the high Pb loading samples. The XAS spectra were therefore strongly dominated by sorbed Pb, with negligible contributions from nonsorbed Pb present in entrained electrolyte.

XAS spectra were recorded on Beamline X-11A of the National Synchroton Light Source at the Brookhaven National Laboratory. All samples were scanned within 48 h following centrifugation. The spectra were collected at the Pb L_{III} edge (13 055 eV) using a Si(111) crystal monochromator detuned by 25% to suppress higher order harmonics. The premonochromator slit width was 0.5 mm. Scanning was done in fluorescence mode at room temperature using a Kr-filled Stern−Heald-type detector equipped with an As filter. At least five scans were collected per sample.

Background subtraction, Fourier filtering, and data fitting were accomplished with the program WinXAS97 (*29*) in combination with the FEFF 7.0 code (*30*). Background absorption was removed by fitting a linear function to the preedge region and a second-order polynomial to the postedge region. The edge-jump was normalized to unity, and the data were converted to k space. The $\chi(k)$-function was extracted using a 5-knot cubic spline function and weighted by k^3. Structural parameters were extracted with fits to the standard EXAFS equation by multishell fitting of the raw k^3-weighted χ spectra. The reference compounds used were Pb^{2+}(aq) and $Pb_4(OH)_4^{4+}$(aq); these references were prepared as described by Strawn and Sparks (*11*). The amplitude reduction factor used in the fitting procedure was 0.65. To reduce the number of free parameters in the fitting procedure, the Debye−Waller factors of all shells were fixed while all other parameters were allowed to float. For the O shells, the values were set at those found for the reference compounds Pb^{2+}(aq) ($\sigma^2 = 0.025$ Å^2) and $Pb_4(OH)_4^{4+}$(aq) ($\sigma^2 = 0.008$ Å^2), which had O shell coordinations similar to those found for the Pb adsorption complexes formed on SiO_2. The Debye−Waller factors of the other shells were fixed at 0.01 Å^2.

The accuracies of the optimized fitting parameters obtained from the fitting procedure were difficult to estimate for a number of reasons. First, the Pb/SiO_2 EXAFS data revealed that two different Pb sorption complexes were simultaneously present at the SiO_2 surface in most samples, as will be shown in the results section. These complexes had different Pb−O shells, separated by about 0.2 Å. Strong correlations between the optimized N_{Pb-O} and R_{Pb-O} values of the first and second O shells resulted. A further complication is that one of the Pb sorption complexes observed had a first-shell O coordination shell similar to that of Pb^{2+}(aq), which has a not-well-characterized first ligand O shell with a high Debye−Waller factor, indicating a high degree of disorder. Fitting the O shell of these complexes with a third cumulant (C_3) term, as done by O'Day et al. (*31*) for Sr^{2+}(aq), did not improve the fit and did not change the fit parameters and was therefore not used in the final analysis. In samples dominated by a single Pb adsorption species, errors are estimated to be ±15% and ± 0.02 Å for the N and R values of the first ligand O shell, respectively, and ±30% and ±0.04 Å for the N and R values of shells located beyond the first coordination shell, which are typical errors for EXAFS data of Pb sorption complexes on mineral surfaces (e.g., refs *4*, *24*, and *25*). The accuracies for samples with two adsorbed Pb species present will be poorer, especially for the O shell parameters.

Results and Discussion

pH Edges. Figure 1 compares the Pb/SiO_2 pH edges of the $I = 0.1$ M $NaClO_4$ and the $I = 0.005$ M $NaClO_4$ systems. Clearly, there is an ionic strength effect, with higher Pb sorption at $I = 0.005$ M over most of the pH range. A similar ionic strength effect on metal sorption to SiO_2 has been reported in uptake studies for other elements (*32*−*35*). This type of ionic strength dependence suggests the presence of Pb sorption complexes with a relatively large component of electrostatic bonding as opposed to chemical bonding, for instance, electrostatically held outer-sphere complexes or weakly bound inner-sphere complexes. Since the Na^+ ions present in the background electrolyte can compete with such metal sorption complexes for sorption sites, there will be less metal sorption when the ionic strength (and therefore the Na^+ concentration) is raised. In a study of Pb sorption to montmorillonite, a strongly swelling clay mineral, Strawn and Sparks (*11*) reported strongly ionic strength-dependent Pb sorption and used EXAFS to demonstrate the importance of Pb outer-sphere complexation at low ionic strength. Similarly, Papelis and Hayes (*7*) used EXAFS to demonstrate the importance of outer-sphere Co complexes on montmorillonite at low ionic strength, explaining increased Co sorption as I was lowered. To characterize the Pb sorption complexes formed in our

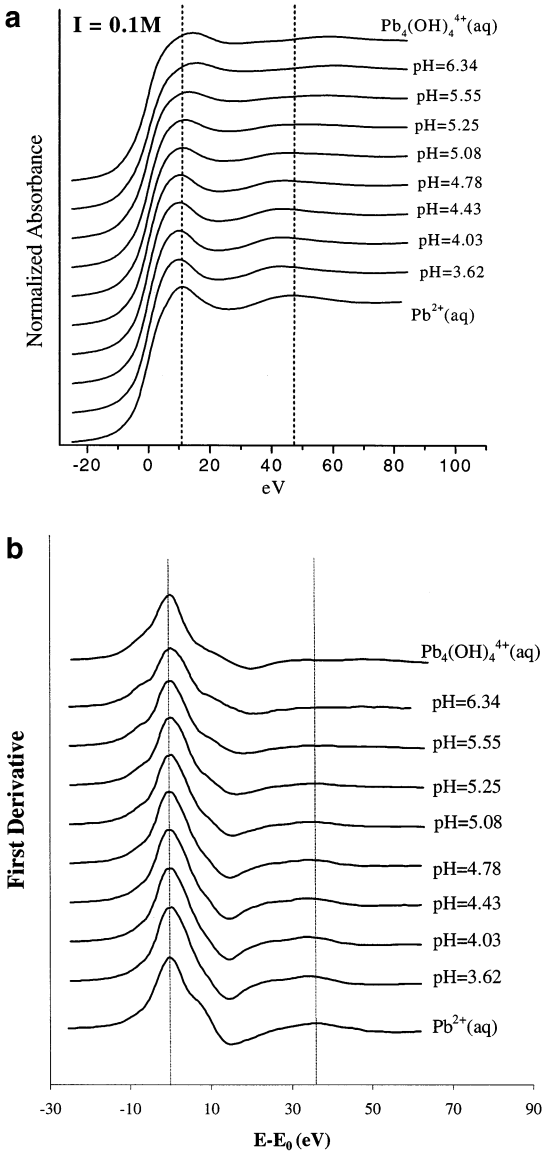

FIGURE 2. (a) Normalized XANES spectra of the $I = 0.1$ M Pb/SiO_2 samples and the Pb^{2+}(aq) and $Pb_4(OH)_4^{4+}$(aq) reference compounds and (b) first derivatives of these spectra.

Pb/SiO_2 system, we performed XAS analyses of Pb/SiO_2 samples reacted over a range of pH values at $I = 0.1$ and 0.005 M. The XAS samples are indicated by arrows in Figure 1 and span the pH range between 3.6 and 7.5.

Near-Edge Spectra. Figure 2 presents the normalized near-edge spectra and their first derivatives of the $I = 0.1$ M XAS samples along with those of the reference compounds Pb^{2+}(aq) and $Pb_4(OH)_4^{4+}$(aq). Samples with low pH (3.5−4.5) have near-edge spectra that are similar, although not identical, to free Pb^{2+}(aq), suggesting that the dominant sorbed Pb species at low pH values have first O ligand shells similar to those of aqueous Pb^{2+} atoms. As pH increases beyond pH 4.5 to pH 6.3, the Pb/SiO_2 spectra increasingly resemble that of $Pb_4(OH)_4^{4+}$(aq). Between pH 4.5 and pH 5.6, the Pb/SiO_2 spectra appear to be intermediate between the spectra of low pH samples and the $Pb_4(OH)_4^{4+}$(aq) reference compound; these spectra could be fit with linear combinations of the low pH and $Pb_4(OH)_4^{4+}$(aq) near-edge spectra (not shown). The Pb/SiO_2 spectra at pH 6.3 and 7.5 are very similar to the spectrum of $Pb_4(OH)_4^{4+}$. The Pb atoms in $Pb_4(OH)_4^{4+}$ have a distorted trigonal pyramidal coordination environment with hydroxide ions as coordinating ligands (*2*). This Pb coordination environment is typical of Pb present

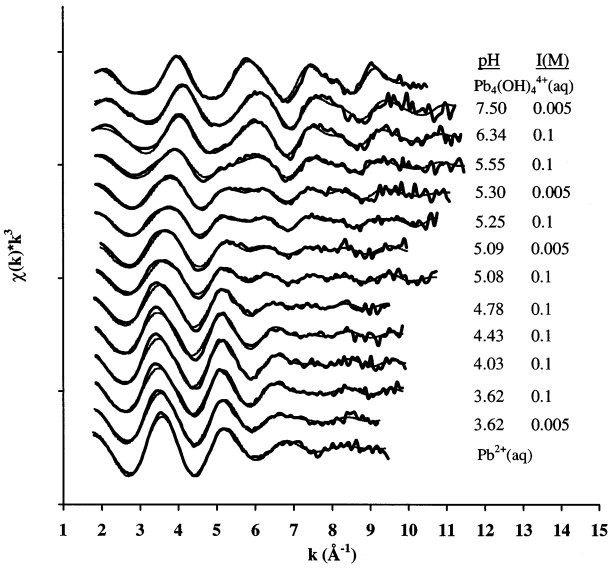

FIGURE 3. Raw k^3-weighted χ spectra of the Pb/SiO_2 samples and aqueous reference compounds analyzed by EXAFS, along with the theoretical χ spectra obtained from data fitting (thin lines).

in a covalent bonding state and has been observed for Pb inner-sphere adsorption complexes at iron, manganese, and aluminum oxide surfaces (*2*−*6*) as well as for multinuclear Pb complexes forming at the montmorillonite surface (*11*). The increasing resemblance between $Pb_4(OH)_4^{4+}$ and Pb/SiO_2 spectra with increasing pH therefore indicates the formation of Pb inner-sphere adsorption complexes and/or multinuclear Pb complexes at the SiO_2 surface as pH increases.

EXAFS Data. The k^3-weighted χ spectra determined from extended X-ray absorption spectroscopy (EXAFS) analyses of the samples are presented in Figure 3 along with the best fits obtained from the fitting procedure. The χ structures show distinct changes as pH increases from 3.6 to 7.5. The low pH spectra are dominated by O shell backscattering resembling that of the Pb^{2+}(aq) reference compound, as expected based on the near-edge spectra discussed above. The signal amplitude of these samples strongly decreases at $k > 8$ Å^{-1}, indicating high structural and thermal disorder and a lack of heavy backscatterers in the second coordination shell of the sorbed Pb metal cations. As pH increases, pronounced features appear in the higher k range, consistent with the presence of heavy backscatterers in the local coordination environment of sorbed Pb.

To isolate the frequencies appearing in the χ spectra presented in Figure 3, the k^3-weighted spectra were Fourier transformed. The resulting radial structure functions (RSFs) are shown in Figure 4. A broad first-shell O peak is observed for the low pH samples along with a small second-neighbor shell. Between pH 4.5 and pH 5.5, a second O shell appears in the RSFs at a shorter radial distance than the O shell observed in the low pH samples. This O shell becomes more pronounced with increasing pH and is the dominant O shell at pH > 6.3. At pH > 4.5, two features appearing at about 3.2 Å (overlapping with the Si shell) and 3.8 Å in the RSFs indicate Pb−Pb scattering and thus the formation of polynuclear Pb complexes in this pH range.

The EXAFS fitting results are presented in Table 1. At low pH, reasonable fits were obtained by fitting two shells: a Pb−O and a Pb−Si shell. The optimized R_{Pb-O} values of these samples ($R_{Pb-O} = 2.5$ Å) are similar to the R_{Pb-O} of the Pb^{2+}-(aq) standard ($R_{Pb-O} = 2.49$ Å). This value along with the high N_{Pb-O} and Debye−Waller factor found for this shell is similar to previously reported values for outer-sphere Pb sorption

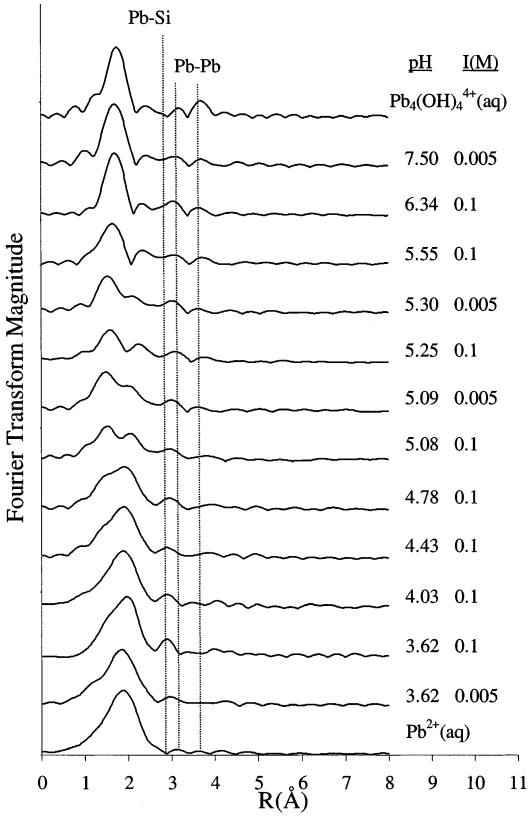

FIGURE 4. Radial structure functions (not corrected for phase shift) obtained by Fourier transforming the raw k^3-weighted χ spectra presented in Figure 3.

TABLE 1. Structural Parameters Derived from EXAFS Data Fitting for the Pb/SiO_2 Sorption Samples and the Aqueous Pb Standards[a]

		long Pb−O[b]		short Pb−O[b]		Pb−Si[b]		Pb−Pb[b]	
I (M)	pH	*N*	*R* (Å)	*N*	*R* (Å)	*N*	*R* (Å)	*N*	*R* (Å)
0.005	7.34			2.2	2.26	0.7	3.43	0.7	3.74
0.1	6.34			2.1	2.27	0.9	3.42	0.7	3.74
0.1	5.55	2.4	2.53	1.8	2.28	0.6	3.44	0.6	3.74
0.005	5.30	3.5	2.48	1.3	2.26	0.9	3.44	0.7	3.70
0.1	5.25	3.8	2.53	1.4	2.29	0.8	3.42	0.8	3.78
0.005	5.09	4.4	2.48	1.0	2.26	0.8	3.42		
0.1	5.08	4.7	2.50	1.0	2.26	0.9	3.42		
0.1	4.78	5.8	2.51	0.4	2.29	0.8	3.43		
0.1	4.43	6.3	2.51			0.8	3.41		
0.1	4.03	6.7	2.52			0.9	3.40		
0.1	3.62	7.3	2.53			1.0	3.41		
0.005	3.62	6.1	2.49			0.6	3.42		
Pb^{2+}(aq)		7.6	2.49						
$Pb_4(OH)_4^{4+}$(aq)				2.2	2.28			1.7	3.77

[a] *N* is the coordination number; *R* is the radial distance. [b] The Debye−Waller factors of the long and short Pb−O shells were fixed at 0.025 and 0.008 Å^2, respectively. The Debye−Waller factors of the Pb−Si and Pb−Pb shells were fixed at 0.01 Å^2.

complexes (*1*, *11*). The long R_{Pb-O} radial distance is typical of Pb present in an ionic bonding state (*2*). Figure 5a presents the Pb−O and Pb−Si shell contributions to the experimental RSF of the pH 4.03 sample ($I = 0.1$ M), as determined from the fitting procedure. The Si shell is not very pronounced in the RSFs of the pH < 4.5 samples (Figures 4 and 5a), and the Si scattering in these samples is more readily observed in the k^3-weighted χ structures shown in Figure 4, which show differences between the χ values of the samples reacted at pH < 4.5 and that of the aqueous Pb^{2+} reference sample, most notably at $k > 6$ Å^{-1}. Differences between the low pH

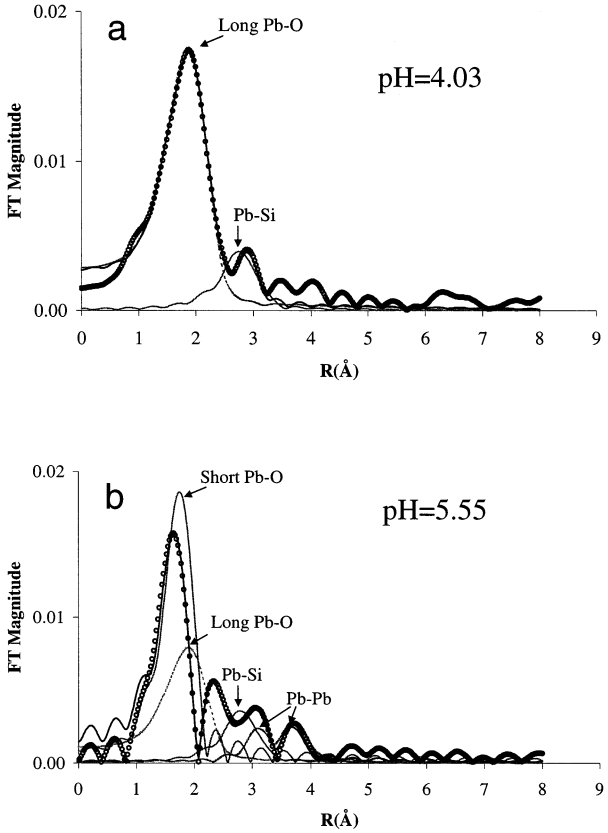

FIGURE 5. Raw (dots) and fitted (black lines) transform magnitudes, and the contributions of the constituting shells (gray lines) for the pH 4.03 (a) and pH 5.55 (b) samples reacted at $I = 0.1$ M.

Pb/SiO_2 samples and the Pb^{2+}(aq) reference compound are also visible in the near-edge spectra (Figure 2). In contrast, Strawn and Sparks (*11*) showed that outer-sphere Pb(II) complexes, held by strictly electrostatic interactions on montmorillonite clay, had χ structures and near-edge spectra identical to that of aqueous Pb^{2+}.

The simultaneous presence of a Si shell and an O shell similar to the O shell of aqueous Pb^{2+}(aq) in the RSFs of the low pH samples may indicate that Pb sorption in this pH region occurs as a mixture of outer-sphere and inner-sphere complexes. The point of zero charge of amorphous silica and quartz is 2−3 (*36*). Therefore, at the pH values used in this study (>3.5), the SiO_2 surface is negatively charged, allowing for the possibility of outer-sphere complexation of Pb^{2+} cations. A measure for the capacity for outer-sphere complexation is provided by the cation exchange capacity (CEC), which was determined as a function of pH for the SiO_2 sorbent used in this study by Huang and Rhoads (*26*) with a modified ammonium acetate method. The Pb surface loadings achieved at pH < 4.5 are about a factor 50 and 100 (for $I = 0.1$ and 0.005 M, respectively) than the silica CEC value in this pH range. This suggests that strictly electrostatic interactions between Pb and the SiO_2 surface cannot account for Pb uptake in this pH region. However, since the CEC determined with divalent exchange cations (Pb in this case) is higher than with monovalent cations (ammonium in the CEC measurements) at a given surface potential value (*37*), this argument is not conclusive. If there is a mixture of inner- and outer-sphere complexes at the SiO_2 surface below pH 4.5 and the inner-sphere complexes have distorted trigonal O ligand shells, as observed for the Pb inner-sphere complexes forming on iron, manganese, and aluminum oxides (*2*−*6*), their R_{Pb-O} would be shorter by about 0.2 Å than the R_{Pb-O} of the outer-sphere complexes. However, attempts to fit a small number of O atoms at a radial distance of 2.20−2.35

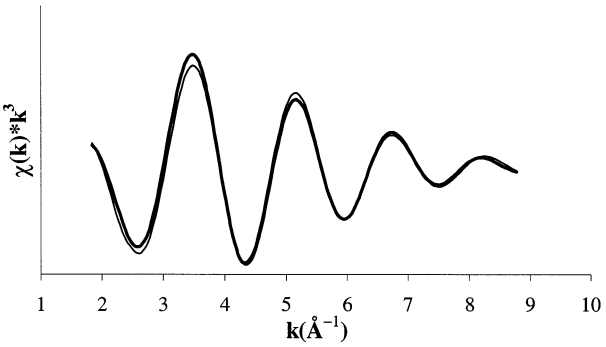

FIGURE 6. Raw (thick line) and fitted (thin line) oxygen contribution to the experimental k^3-weighted χ spectrum of the sample reacted at pH 4.03 and $I = 0.1$ M isolated by backtransforming the O shell in the RSF.

Å failed, and isolating the O contributions by backtransforming the O shell in the RSF over $k = 0.5-2.4$ Å^{-1} showed no indication of an additional O shell with shorter R_{Pb-O}, as indicated by the agreement between the raw backtransformed data and the fit obtained with a single O shell (Figure 6). To test the possiblity of H-bonding between hydrated Pb cations and surface silanol groups, we also attempted to fit the second shell in these samples with O scattering, but this failed to produce good fits of the experimental spectra. We conclude that Pb sorption in the pH < 4.5 region does not occur as a mixture of inner- and outer-sphere complexes or through H-bonding between hydrated Pb cations and surface functional groups. Rather, the combined information obtained from the macroscopic (Figure 1) and spectroscopic data appears to indicate the presence of an ionic inner-sphere Pb sorption complex in the low pH range where Pb is coordinated to SiO_2 surface sites while having a similar oxygen coordination shell it has as a free ion in solution, with one or two water ligands exchanged for surface (hydr)oxide ligands. This interpretation is consistent with the results of Fitts et al. (*38*), who concluded based on grazing incidence studies that, at pH 5.0, Cu(II) forms mononuclear inner-sphere complexes on silica that are weakly bound to the surface as compared to the mononuclear inner-sphere Cu(II) sorption complexes forming at the Al_2O_3 surface. In an EXAFS study of U(VI) sorption to amorphous silica, Sylwester et al. (*39*) report mononuclear inner-sphere complexation of UO_2^{2+} on amorphous SiO_2 at a pH value as low as 3.14.

The spectra of the samples reacted in the pH range 4.5−5.5 all required two O shells to obtain reasonable fits (Table 1). The first O shell had the same radial distance as the dominant O shell present in samples reacted below pH 4.5 ($R_{Pb-O} = 2.5$ Å), and the second O shell had a R_{Pb-O} of about 2.28 Å, which is consistent with Pb coordinated by three O ligands in a distorted trigonal configuration and indicates that Pb is present in a covalent bonding state (*2, 40*). These findings indicate the simultaneous presence of two different Pb sorption complexes at the SiO_2 surface in the pH range 4.5−5.5: the ionic inner-sphere complex that dominates at low pH (with $R_{Pb-O} = 2.5$ Å) and a more covalent Pb sorption complex ($R_{Pb-O} = 2.3$ Å). Inspection of the RSFs in Figure 4 and the fitting results presented in Table 1 shows that the formation of Pb sorption complex with the shorter R_{Pb-O} distance ($R_{Pb-O} = 2.3$ Å) increases relative to the surface complex with the longer Pb−O radial distance ($R_{Pb-O} = 2.5$ Å) as pH increases. Besides the two O shells, a Si shell at 3.45 Å was required to obtain good fits for these samples. Moreover, for the pH 5.25 and pH 5.55 samples, Pb−Pb scattering also had to be included for a good fit (Table 1). Although the RSF of the sample reacted at pH 5.1 also shows evidence of Pb−Pb scattering, it was too minor to improve the quality of the fit when included in the fitting procedure. Figure 5b shows the contributions of the two Pb−O shells; the Pb−Si and the Pb−Pb shells for the experimental RSF of the sample reacted at pH 5.55. Note that because of the specific backscattering characteristics of Pb, the presence of a single Pb shell is indicated by two features in the RSF. The samples reacted at pH 6.3 and 7.5 show only the O shell with $R_{Pb-O} = 2.28$ Å (Figure 4 and Table 1). Additional scattering in these samples resulted from the presence of Si and Pb in the local coordination environment of sorbed Pb at radial distances also found in the other samples (Table 1).

The combined XANES and EXAFS analyses point to a strong pH effect on the Pb sorption mechanism to amorphous SiO_2. At pH < 4.5, a mononuclear inner-sphere Pb sorption complex of ionic character dominates. As pH increases from 4.4 to 6.3, the importance of this sorption complex decreases, and a more covalent Pb sorption complex becomes increasingly important until it is the dominant Pb surface species at pH > 6.3. The simultaneous appearance of the shorter Pb−O and Pb−Pb bonds suggests that the covalent Pb sorption complexes forming when pH is raised are multinuclear Pb complexes, possibly Pb−Pb dimers. This is consistent with EXAFS studies of Cu(II), Ni(II), Co(II), and Cr(III) sorption on SiO_2, all of which were performed at pH > 5.5 and reported the formation of multinuclear hydroxide like sorption products for these metals when contacted with SiO_2 at similar metal loadings (*10, 16−23*). The presence of Si backscattering at pH > 6 indicates that the Pb multinuclear complexes are attached to the SiO_2 surface via inner-sphere bonds, which was also found for Cr(III) and Cu(II) polymers forming at the amorphous SiO_2 surface (*11, 15*) as well as for Pb polymers sorbed on alumina (*2*). The small degree of Pb−Pb scattering relative to the $Pb_4(OH)_4^{4+}$ reference compound suggests that the polymers are small and that no extensive sheets of lead phyllosilicates are formed, as has been reported by Manceau et al. (*16*) in the case of Co(II) sorption to quartz. Differences between Co(II) and Pb(II) with respect to the sorption complexes formed on mineral surfaces also occur when these metals are reacted with Al-containing phyllosilicates and aluminum oxides. In such systems, Co(II) forms mixed cobalt−aluminum hydroxide precipitate phases at near-neutral pH (*41*), whereas Pb(II) forms mononuclear adsorption complexes and/or surface attached dimers under similar conditions (*2, 4*). The concentration of silica sites in our systems is 18 mM, as calculated based on an active site density of 5.5 sites nm^{-2} (*42*), whereas Pb polymerization is observed at Pb uptake of ∼1 mM. This suggests that saturation of surface sites with Pb is not the reason for the observed formation of polynuclear Pb complexes.

While pH has a strong effect on the mechanism of Pb sorption to the amorphous SiO_2 surface, the ionic strength does not appear to strongly influence the average local coordination environment of sorbed Pb at a given pH, as shown by the similarity in the χ structures and RSFs of low and high I samples reacted at similar pH values (Figures 3 and 4). Therefore, the increase in Pb sorption observed when lowering the ionic strength from $I = 0.1$ M to $I = 0.005$ M (Figure 1) is due to increases in both the mononuclear and the polynuclear Pb sorption complexes forming at the amorphous SiO_2 surface, in roughly equal amounts. This suggests a coupling between mononuclear and polynuclear Pb sorption complex formation at the silica surface. The formation of Pb surface polymers at a given pH value may be controlled by diffusion of Pb monomers along the surface. Another possibility is that the mononuclear sorption complexes act as nucleation centers when additional Pb uptake from solution takes place. Coupling of monomer and polymer formation was also noted in an EXAFS study by Fitts et al. (*43*) in the case of Cr(III) sorption to γ-alumina and in the case of Cu(II) sorption to SiO_2 by Cheah et al. (*23*). The results

of Cheah et al. (*23*) support the idea that metal polymer formation is at least partially controlled by diffusion of monomers along the SiO_2 surface. In this EXAFS study of Cu sorption on amorphous SiO_2, the fraction of Cu polymers was found to increase at the expense of Cu monomers within the same sample at longer contact times. Additional Cu uptake from solution could not explain this observation since the samples had been centrifuged. The results therefore indicated a transformation of Cu monomers into Cu polymers at the SiO_2 surface, suggesting that monomers had diffused along the surface and formed polymers. Unlike for sorption of Pb(II) on SiO_2, lowering *I* in the case of Pb(II) and Co(II) sorption to montmorillonite has been shown to dominantly favor ionic (outer-sphere) metal complexation (*7*, *11*). The difference between amorphous SiO_2 versus montmorillonite in this respect likely is due to the strong separation of inner- and outer-sphere sites on montmorillonite, where sites for outer-sphere sorption are located in the internal surface area of the clay, and inner-sphere sorption sites are located on the clay edges, whereas at the amorphous SiO_2 surface, such a strong spatial separation of sites does not exist. Increasing the concentration of ionic mononuclear Pb sorption complexes at the SiO_2 surface by lowering the ionic strength at a given pH value may then, via mass action, drive additional Pb−Pb polymerization as well.

It is interesting to note that the EXAFS data results indicate that, while the Pb first shell O coordination changes drastically with pH, the optimized R_{Pb-Si} values remain essentially the same (Table 1), although it should be noted that due to the overlap with the Pb−Pb shells, the Pb−Si fitting parameters of the high pH samples are less accurate than those of the low pH samples. Nevertheless, these results suggest that the conversion of mononuclear species into Pb polymers involves not only a change in the O coordination but also a rearrangement in the surface coordination, resulting in similar Pb−Si distances for mononuclear and polynuclear Pb sorption complexes. A similar observation was made by Bochatay and Persson (*44*) in an EXAFS study of Zn sorption to manganite. With increasing pH, sorbed Zn was found to change from predominantly mononuclear (inner-sphere) species octahedrally coordinated by O into polynuclear Zn species with tetrahedral O coordination, without a significant change in the R_{Zn-Mn} distance. The R_{Pb-Si} distance of 3.45 Å indicates that the Pb sorption complexes are coordinated in a monodentate or bridging bidentate fashion to SiO_4 surface tetrahedra. Coordination of Pb to the edges of SiO_4 tetrahedra would result in considerably shorter R_{Pb-Si} values (2.8−3.0 Å) and probably is not favored due to the strong $Si^{4+}-Pb^{2+}$ repulsion in this configuration. The exact mechanism of Pb monomers transforming into Pb surface polymers cannot be extracted from our data, but a possible scenario is that Pb monomers bound to SiO_4 tetrahedra in a bridging bidentate coordination via long Pb−O bonds transform into clustered Pb species linked via short Pb−O bonds to Si and Pb atoms in a monodentate fashion, similar to the configuration of Cu−Cu dimers at the SiO_2 surface proposed by Cheah et al. (*23*).

Literature Cited

(1) Bargar, J. R.; Towle, S. N.; Brown, G. E., Jr.; Parks, G. A. *Geochim. Cosmochim. Acta* **1996**, *60*, 3541−3547.
(2) Bargar, J. R.; Brown, G. E., Jr.; Parks, G. A. *Geochim. Cosmochim. Acta* **1997**, *61*, 2617−2637.
(3) Bargar, J. R.; Brown, G. E., Jr.; Parks, G. A. *Geochim. Cosmochim. Acta* **1997**, *61*, 2639−2652.
(4) Strawn, D. G.; Scheidegger, A. M.; Sparks, D. L. *Environ. Sci. Technol.* **1998**, *32*, 2596−2601.
(5) Scheinost, A. C.; Abend, S.; Pandya, K. I.; Sparks, D. L. *Environ. Sci. Technol.* **2001**, *35*, 1090−1096.
(6) Matocha, C. J.; Elzinga, E. J.; Sparks, D. L. *Environ. Sci. Technol.* **2001**, *35*, 2967−2972.
(7) Papelis, C.; Hayes, K. F. *Colloids Surf.* **1996**, *107*, 89−96.
(8) Towle, S. N.; Bargar, J. R.; Brown, G. E., Jr.; Parks, G. A. *J. Colloid Interface Sci.* **1997**, *187*, 62−82.
(9) Scheidegger, A. M.; Strawn, D. G.; Lamble, G. M.; Sparks, D. L. *Geochim. Cosmochim. Acta* **1998**, *62*, 2233−2245.
(10) Xia, K.; Taylor, R. W.; Bleam, W. F.; Helmke, P. A. *J. Colloid Interface Sci.* **1998**, *199*, 77−82.
(11) Strawn, D. G.; Sparks, D. L. *J. Colloid Interface Sci.* **1999**, *216*, 257−269.
(12) Ford, R. G.; Sparks, D. L. *Environ. Sci. Technol.* **2000**, *34*, 2479−2483.
(13) Scheckel, K. G.; Scheinost, A. C.; Ford, R. G.; Sparks, D. L. *Geochim. Cosmochim. Acta* **2000**, *64*, 2727−2735.
(14) Ford, R. G.; Scheinost, A. C.; Scheckel, K. G.; Sparks, D. L. *Environ. Sci. Technol.* **1999**, *33*, 3140−3144.
(15) Berner, R. A. *Principles of Chemical Sedimentology*; McGraw-Hill Book Company: New York, 1971.
(16) Manceau, A.; Schlegel, M.; Nagy, K. L.; Charlet, L. *J. Colloid Interface Sci.* **1999**, *220*, 181−197.
(17) d'Espinose de la Caillerie, J. B.; Kermarec, M.; Clause, O. *J. Phys. Chem.* **1995**, *99*, 17273−17281.
(18) Charlet, L.; Manceau, A. *Geochim. Cosmochim. Acta* **1994**, *58*, 2577−2582.
(19) Fendorf, S. E.; Lamble, G. M.; Stapleton, M. G.; Kelley, M. J.; Sparks, D. L. *Environ. Sci. Technol.* **1994**, *28*, 284−289.
(20) O'Day, P. A.; ChisholmBrause, C. J.; Towle, S. N.; Parks, G. A.; Brown, G. E., Jr. *Geochim. Cosmochim. Acta* **1996**, *60*, 2515−2532.
(21) Xia, K.; Mehadi, A.; Taylor, R. W.; Bleam, W. F. *J. Colloid Interface Sci.* **1997**, *185*, 252−257.
(22) Scheinost, A. C.; Ford, R. G.; Sparks, D. L. *Geochim. Cosmochim. Acta* **1999**, *63*, 3193−3203.
(23) Cheah, S. F.; Brown, G. E., Jr.; Parks, G. A. *J. Colloid Interface Sci.* **1998**, *208*, 110−128.
(24) Ostergren, J. D.; Trainor, T. P.; Bargar, J. R.; Brown, G. E., Jr.; Parks, G. A. *J. Colloid Interface Sci.* **2000**, *225*, 466−482.
(25) Ostergren, J. D.; Brown, G. E., Jr.; Parks, G. A.; Persson, P. *J. Colloid Interface Sci.* **2000**, *225*, 483−493.
(26) Huang, C. P.; Rhoads, E. A. *J. Colloid Interface Sci.* **1988**, *131*, 289−306.
(27) Schulthess, C. P.; Huang, C. P. *Soil Sci. Soc. Am. J.* **1990**, *54*, 679−688.
(28) Schecher, W. D. *MINEQL+ Version 3.01b*; Environmental Research Software: Hallowell, ME, 1994.
(29) Rehr, J. J.; Mustre de Leon, J. M.; Zabinsky, S. I.; Albers, R. C. *J. Am. Chem. Soc.* **1991**, *113*, 5135−5140.
(30) Ressler, T. *J. Phys. IV* **1997**, *7*, 269−270.
(31) O'Day, P. A.; Newville, M.; Neuhoff, P. S.; Sahai, N.; Carroll, S. A. *J. Colloid Interface Sci.* **2000**, *222*, 184−197.
(32) Kosmulski, M. *J. Colloid Interface Sci.* **1997**, *190*, 212−223.
(33) DeGueldre, C.; Wernli, B. *J. Environ. Radioact.* **1993**, *20*, 151−167.
(34) Csoban, K.; Parkanyi-Berka, M.; Joo, P.; Behra, P. *Colloids Surf.* **1998**, *141*, 347−364.
(35) Kitamura, A.; Yamamoto, T.; Moriyama, H.; Nishikawa, S. *J. Nucl. Sci. Technol.* **1996**, *33*, 840−845.
(36) Parks, G. A. *Chem. Rev.* **1965**, *65*, 177−198.
(37) Bolt, G. H. In *Soil Chemistry A. Basic Elements*; Bolt, G. H., Bruggenwert, M. G. M., Eds.; Elsevier Publishing: Amsterdam, 1978.
(38) Fitts, J. P.; Trainor, T. P.; Grolimund, D.; Bargar, J. R.; Parks, G. A.; Brown, G. E., Jr. *J. Synchrotron Radiat.* **1999**, *6*, 627−629.
(39) Sylwester, E. R.; Hudson, E. A.; Allen, P. G. *Geochim. Cosmochim. Acta* **2000**, *64*, 2431−2438.
(40) Manceau, A.; Boisset, M. C.; Sarret, G.; Hazemann, J. L.; Mench, M.; Cambier, P.; Prost, R. *Environ. Sci. Technol.* **1996**, *30*, 1540−1552.
(41) Thompson, H. A.; Parks, G. A.; Brown, G. E., Jr. *Geochim. Cosmochim. Acta* **1999**, *63*, 1767−1779.
(42) Fouad, N. E.; Knozinger, H.; Zaki, M. I.; Mansour, S. A. A. *Z. Phys. Chem.* **1991**, *171*, 75−96.
(43) Fitts, J. P.; Brown, G. E., Jr.; Parks, G. A. *Environ. Sci. Technol.* **2000**, *34*, 5122−5128.
(44) Bochatay, L.; Persson, P. *J. Colloid Interface Sci.* **2000**, *229*, 593−599.

Received for review December 18, 2001. Revised manuscript received July 15, 2002. Accepted August 5, 2002.

ES0158509